CHALMERS
UNIVERSITY OF TECHNOLOGY

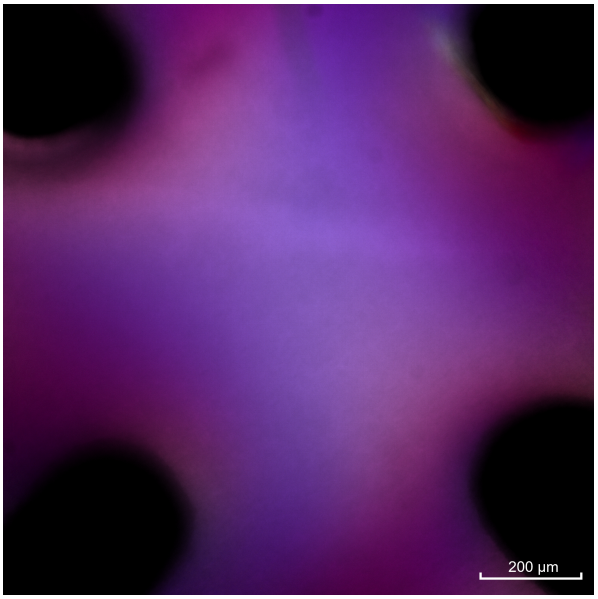

Investigation of the effect of complex flow fields on cellulose nanofibril suspensions by birefringence imaging

Master's thesis in Applied Physics

SARA-LOUISE KARLSSON

DEPARTMENT OF PHYSICS

CHALMERS UNIVERSITY OF TECHNOLOGY
Gothenburg, Sweden 2020
www.chalmers.se

Master's thesis 2020

Investigation of the effect of complex flow fields on cellulose nanofibril suspensions by birefringence imaging

SARA-LOUISE KARLSSON

CHALMERS
UNIVERSITY OF TECHNOLOGY

Department of Physics
Division of Materials Physics
Liebi research group
Chalmers University of Technology
Gothenburg, Sweden 2020

Investigation of the effect of complex flow fields on cellulose nanofibril suspensions by birefringence imaging
SARA-LOUISE KARLSSON

Supervisor: Barbara Berke, Department of Physics
Examiner: Marianne Liebi, Department of Physics

Master's Thesis 2020
Department of Physics
Division of Materials Physics
Liebi research group
Chalmers University of Technology
SE-412 96 Gothenburg
Telephone +46 31 772 1000

Cover: A combined image of the intensity, retardance and angle of the fast axis from a measurement with a 0.25 wt% cellulose nanofibril suspension in extensional flow with flow rate $Q_1 = 20\,\mu L/s$, recorded with the Exicor Birefringence MicroImager.

Typeset in LaTeX
Printed by Chalmers Reproservice
Gothenburg, Sweden 2020

Investigation of the effect of complex flow fields on cellulose nanofibril suspensions by birefringence imaging
SARA-LOUISE KARLSSON
Department of Physics
Chalmers University of Technology

Abstract

Cellulose is an interesting renewable material with many unique properties. A type of nanocellulose is cellulose nanofibrils (CNF). It has potential to be used as reinforcement in composites, to modify the rheology of complex systems in 3D printing and in fiber production, among other areas. They are relatively long and flexible particles with both crystalline and amorphous parts. This material can be used to make stronger materials by increasing the alignment of the fibrils. In all of these cases, it is crucial to understand the behavior of the material in flow, which is the focus of this thesis.
The aim with this project is to study how the alignment in cellulose nanofibril suspensions is affected in different flow types (extensional, shear and two mixed flow types), how it changes with different flow rates (1 - 50 µL/s) and if it is affected by the concentration of the suspensions (0.1, 0.25 and 0.5 wt%). To achieve the different complex flow fields, a fluidic four-roll mill was used. The alignment of the nanofibers were then determined by a birefringence imager which measured the retardance, angle of the fast axis and the intensity.
The results showed that the used setup with the fluidic four-roll mill and birefringence imager can successfully measure the alignment in CNF suspensions, and that the experiments can be performed continuously with any one wavelength. Dependence on the concentration of the suspensions, flow rate and flow type was found. The alignment increased in extensional flow with increasing concentration, but not in shear flow. The flow rate dependence showed that the alignment increased with the flow rate for the highest concentration (0.5 wt%), but did not have much effect on the lowest concentration (0.1 wt%). It was found that extensional flow achieved more alignment than shear flow in the two higher concentrations of suspensions, but that the flow type had less effect in the lowest concentration. An unexpected dependency on the age of the sample and the assembly of the device was also observed.

Keywords: cellulose nanofibrils, fluidic four-roll mill, birefringence imager, alignment.

Acknowledgements

First, I would like to thank my supervisor Barbara Berke for helping me through this thesis work, and being there for all of the discussions and answering many of my questions. I also want to thank Marianne Liebi for being my examiner and contributing with many helpful comments and ideas. I am also thankful to the Liebi Research Group and the entire (K)MF group for being very nice people and creating a great place to work in.
Furthermore I want to give thanks to RISE for providing the 1 wt% CNF suspension which was used as the basis for the suspensions, and to Kristina Stenborgs Stiftelse and Wallenberg Wood Science Center for financial support of the birefringence microscope.
Finally, I also want to thank my friends and family for being there for me and supporting me through my education.

Sara-Louise Karlsson, Gothenburg, June 2020

Contents

List of Figures

1
Introduction

1.1 Background

Cellulose is an abundant natural polymer that is found in plants and wood in nature. In Sweden, forests cover more than half of the land area, 57% [1]. From cellulose, nanocellulose can be derived, which has many unique properties that make it an interesting material as well as a building block for new materials. It is strong, lightweight and renewable since it is derived from plants. Nanocellulose is an environmentally friendly material, a good alternative for some currently used ones [2]. To be able to use it in different applications it needs to be studied to learn more about its properties and how it behaves in different environments or under different conditions.

Nanocellulose has become more and more studied in the last decade, with about 4500 patents published between 2010 and 2017 related to nanocellulose, with 70% of these patents published between 2015 and 2017. There are different types of nanocellulose materials, based on how they are obtained, for example cellulose nanocrystals (CNC), cellulose nanofibrils (CNF) and bacterial nanocellulose (BNC). (More about CNC and CNF is discussed in the theory chapter, Section 2.1.) Patents have been submitted to use CNFs in absorbent products, as reinforcement of composite materials, for modifying the rheology of materials, and for use in many papermaking products [3]. As an example, among many, nanocellulose and CNF have interesting applications in 3D printing with medical applications, where they are used to modify the rheology of the 3D printing inks and for their ability to support living cells [4]. The anisotropy of the CNFs and CNCs plays an important role in the characteristics of the produced materials. In another example, CNF is used to make tougher fibers and it is shown that more alignment increases the toughness [5]. In both of these examples, the properties of the materials in flow and the resulted alignment are crucial to control.

Some studies have been made about orientation and alignment of nanocellulose materials in flow, for example about the orientation distribution of CNC and CNF in flow using a straight quadratic channel and SAXS measurements [6], or using birefringence and a flow-focusing channel to look at orientational dynamics of different CNF suspensions [7]. These studies focused on one specific flow type, but more information is still needed on how CNF align depending on the used conditions, such as concentrations of the suspension, flow types and flow rates, which is where this project aims to contribute. The fluidic four-roll mill (FFoRM) device has been used, which can provide a wide range of flow types [8].

1.2 Aim and limitations

The purpose of this project is to study the effect of complex flow fields on cellulose nanofibril suspensions using birefringence imaging. The CNF suspensions of 0.1-0.5 wt% are studied in four different flow types and over the 1-50 µL/s range of flow rates. The main questions to answer are:

- How is the alignment of the fibrils in CNF suspensions affected by the used flow types?
- How does the alignment change in the applied flow rate range?
- Does the concentration of the suspensions affect the achieved alignment?

The limitations in this project come mainly from the limitations in the FFoRM device and the available time frame of the project. Like with any device the FFoRM has limitations on what it can handle and not, this determines the chosen parameter-range. For example there is a maximum limit on the pressure which the device can handle, which consequently also sets a limit on the maximum concentration of suspensions and on the maximum flow rate that can be investigated. The time limit for the project determined the number of experiments that could be performed during the project.

1.3 Structure of the thesis

This thesis is structured in five main chapters. After this first introduction chapter, the second chapter presents some theory about nanocellulose, the FFoRM device and birefringence.
The third chapter presents the methods and materials that have been used in this study. It is presented how the samples were prepared, how the setup looked, how the measurements were made and how the data analysis was done.
Chapter 4 then presents and discusses the results from the measurements and analysis that were made about the alignment depending on the studied parameters. Finally Chapter 5 summarizes the thesis, the conclusions that can be drawn are discussed and some thoughts are given on possible future experiments that can be done.

2
Theory

In this chapter, the theoretical background for the project is presented. An introduction is given to nanocellulose, the studied material, to the fluidic four-roll mill (FFoRM) device, which was used to create different flow fields and to birefringence which was used to obtain information about alignment in the material.

2.1 Cellulose and nanocellulose

Cellulose is a natural polymer built of glucose molecules that is found in the cell walls of plants to provide structure. Nanocellulose is a general name for cellulose on the nanoscale or nanomaterials derived from cellulose. There are many forms of nanocellulose but the two main types are cellulose nanocrystals (CNC) and cellulose nanofibrils (CNF). Cellulose nanocrystals are rigid, rod-like particles with a diameter of about 2-20 nm and a length of 100-500 nm. Cellulose nanofibrils are longer and more flexible particles with both crystalline and amorphous regions with a diameter in the range of 1-100 nm and length of 0.5-2 µm. Cellulose nanocrystals are often derived from cellulose fibrils by chemical methods such as acid hydrolysis to dissolve the amorphous parts and leave the crystalline parts, the nanocrystals. Cellulose nanofibrils are derived by mechanical methods where large forces, for example, high shear can be used to disintegrate the cellulose. The sizes and shapes of both CNC and CNF, however, depends strongly on the starting resource and the conditions during production. This also means that all batches are different and there is polydispersity in the length of the particles that cannot be avoided [9][10].
Using only mechanical methods to produce cellulose nanofibrils requires a lot of energy. Chemical pretreatments such as carboxymethylation or TEMPO-mediated oxidation can be used in order to decrease the amount of energy needed and to fine-tune the surface properties of the produced nanofibrils. Cellulose nanofibrils made with chemical pretreatment are a bit smaller in size than the ones made without, and are charged on their surface so they tend to aggregate less because of electrostatic repulsion. Cellulose nanofibril suspensions with chemical pretreatments are, therefore, more colloidally stable. They form highly viscous suspensions already at low concentrations when the fibrils entangle and form a physical gel. These CNF suspensions are also shear thinning, meaning that their viscosity decreases when the shear rate is increased, and thixotropic, so the viscosity decreases with time for constant shear rates [11].
Depending on the concentration of the suspension, it can be said to be dilute, semi-dilute or concentrated. The gel point is where the CNF suspensions change from

being dilute to a semi-dilute suspension. The crowding number, N, can be used as a measure of the number of interactions for a suspension with elongated particles, calculated as

$$N = \frac{2}{3} C_v \left(\frac{l}{d} \right)^2, \tag{2.1}$$

where C_v is the volume concentration and l and d are the length and diameter of the particles respectively. Here it is seen that the aspect ratio, l/d, has a big effect on the crowding number, and thus the number of interactions. When $N \ll 1$ the suspension is dilute, between $1 < N < 60$ it is semi-dilute and if $N > 60$ it is concentrated. In the dilute regime interactions between the particles can be neglected, however, in the semi-dilute regime particle-particle interactions are more important and in the concentrated regime the particles form a strong network and don't move much [12][13].
Some applications of CNF, as mentioned in the first chapter, Section 1.1, are for example in absorbent products, for reinforcement in composite materials, for modifying the rheology of materials and in papermaking products, among other areas [3]. CNF is interesting to use for its rheological properties in 3D printing with medical applications [4]. It has also been used to make stronger fibers with increased alignment [5].
There are studies that have investigated the alignment properties of nanocellulose in flow. One example studied the alignment of CNF in a flow-focusing channel with SAXS and showed that there was increased order and alignment of fibrils during extensional flow [14]. Another study looked at the orientation distribution in a straight quadratic channel at different flow rates, also with SAXS, and did simulations with the particles as brownian ellipsoids. There the particles aligned by the shear flow along the walls and dilute CNC experiments agreed well with simulations of brownian ellipsoids. Semi-dilute CNC and CNF systems had relatively high alignment already at low flow rates, so the particle interactions are important for alignment. At higher flow rates the alignment seemed to level off [6]. Both of these focused on extensional and shear dominated systems. If one wants to have a detailed overview of the same system a different approach is needed.

2.2 Fluidic four-roll mill

Many devices that are used for studying materials in flow can generate only some flow types. For example, the cross-slot microfluidic device with four opposing channels where two are inlets and two are outlets, can be used for extensional flow with a stagnation point [15]. Another cross-shaped device is the flow-focusing channel that can be used to produce extensional flow in the center. Then there is also the converging channel, where extensional flow is obtained in the center and shear flow closer to the walls [16]. The geometries of these devices are sketched in Figure 2.1. If you want to study other flow types you have to use different devices, but they may not have the completely same conditions so it can be hard to compare the results obtained with different devices. This is where the FFoRM has a big advantage in that it can create any type of 2D flow field, so only one device is needed.

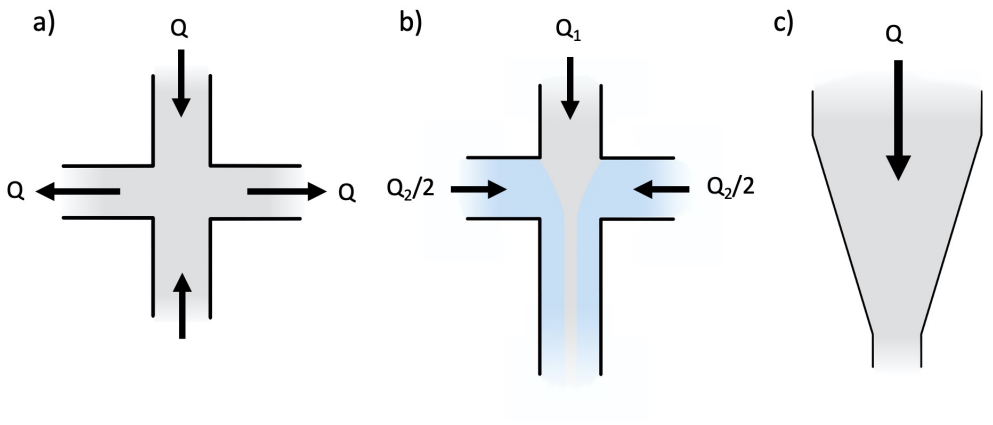

Figure 2.1: Sketches of three devices used to study materials in flow, seen from above. a) a cross-slot microfluidic device, b) a flow-focusing channel and c) a converging channel. Q, Q_1 and Q_2 are flow rates and the arrows indicate their direction.

A four-roll mill uses four cylindrical rollers that are turning and thus is able to generate arbitrary flow fields. Its drawback is that it is too large to use with many optical and scattering measuring methods [17].

The fluidic four-roll mill (FFoRM) uses the same principle as the four-roll mill, but instead of four rollers, it has eight channels. The FFoRM is able to produce complex 2D flow fields alike the flows that appear in real applications, and allow the material to be studied in flow. By changing only the ratio of two flow rates the flow can be varied. It has been shown that the FFoRM can produce complex, stable, homogeneous flows for Newtonian fluids but also for some non-Newtonian fluids and then allow them to be studied with methods like small-angle X-ray and neutron scattering (SAXS, SANS respectively) and birefringence imaging. A simple image showing the geometry of this device is shown in Figure 2.2 [8][17].

The device has eight channels where four are controlled in which the studied material is pumped through with desired flow rates, and the other four are naturally outlets where the flow rates are not controlled. The four channels marked with flow rates Q_1 and Q_2 are the inlets and in Figure 2.2, they are used to push fluid in through the channels marked with Q_1 and pull fluid out through the channels marked with Q_2. When Q_1 and Q_2 are set in this way and are equal in size, extensional flow is obtained. Rotational flow and shear flow are obtained by using the four channels marked with Q_1 and Q_2 as inlets pushing in fluid, with equal flow rates for rotational flow, and larger flow rate Q_1 than Q_2 for shear flow (ratio $Q_2/Q_1 = 0.8$). Other mixed flow types are achieved by changing the direction and the ratio of the flow rates Q_1 and Q_2 to get different combinations of extensional, shear and rotational flow components. So in order to have full control of the flow field only two flow rates, Q_1 and Q_2, and their directions need to be controlled. In the center of the device, the flow is well-defined and the stagnation point is found. This point is in the focus of this project [8].

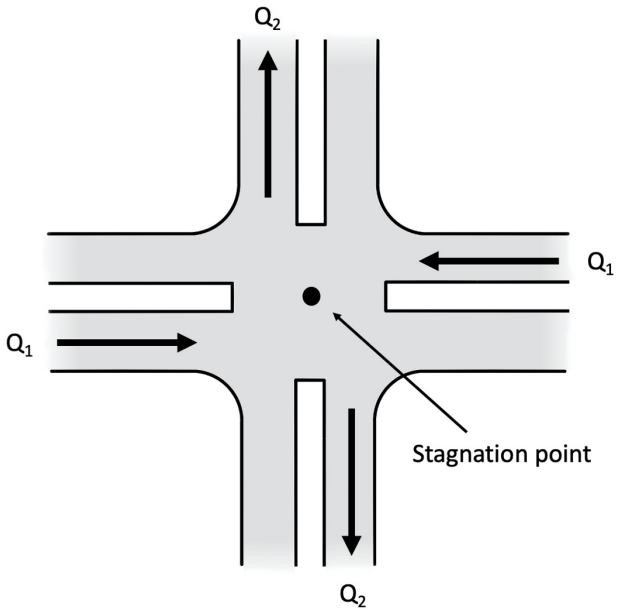

Figure 2.2: The geometry of the FFoRM device, seen from above. Q_1 and Q_2 are the two flow rates that are controlled in four channels. With Q_1 and Q_1 equal in size and with the directions indicated by the arrows, extensional flow is obtained.

2.3 Birefringence

Birefringence is based on the property that some materials can be optically anisotropic, meaning that light can experience different refractive indices depending on the direction with which it travels through the material. When light hits an optically anisotropic material it generally splits into two rays unless it hits the material parallel to the optical axis. This splitting of light is also called double refraction of light. Light that enters through the optical axis of an anisotropic crystal does not experience any birefringence or refraction. However, when it is not parallel to the optical axis the light splits into two rays, the ordinary ray and the extraordinary ray. The ordinary and extraordinary rays have perpendicular polarizations to one another, and experience different refractive indices as they travel through the material. The ordinary ray is called ordinary since it will travel through the material as normal and experience a refractive index that is only dependent on the material. The extraordinary ray however will experience a refractive index that is also dependent on the direction of propagation. The two rays therefore travel through the material with different velocities and will have a phase difference when they leave the material. This phase difference is the retardance and is measured in length units, like nanometers. Birefringence is the difference between the refractive indices experienced by the ordinary and extraordinary rays. The retardance Γ and birefringence B are related as

$$\Gamma = t \cdot B = t \cdot |n_e - n_o| \,, \tag{2.2}$$

where t is the thickness of the material and n_e and n_o are the refractive indices experienced by the extraordinary and ordinary rays, respectively. This also means

that the light will have a different polarization when it exits the sample compared to before it entered the sample. The axis through the material where light travels the fastest is called the fast axis [18][19].
Birefringence in materials can be caused by different things. There is intrinsic birefringence which is attributed to the properties of the molecules that the material is made of, like in anisotropic crystals where the birefringence appears because the atoms are organized in a crystal structure. There is also form birefringence which is caused by orderly arrangement of larger objects than molecules or atoms. For example, a system of parallel rods will show form birefringence. It also depends on the difference between the refractive index of the material and the refractive index of the medium that the material is in. If the refractive index of the medium and of the material are the same no birefringence is observed [20]. Birefringence can be induced on materials by applied stress, strain, or flow for example, e.g., by outer forces that align the rods or molecules. This allows us to measure the alignment in a material with birefringence, the more aligned the particles in a material are the more birefringent signal it will show.
Samples can show both intrinsic and form birefringence, so the birefringence that is measured is then a combination of both [20]. CNF suspensions show increase in birefringence with the alignment of the fibrils [14][16].
Birefringence can be determined by measuring the polarization of light that has passed through a birefringent sample. A simple way of doing this is by using two polarizers at 90° with the sample placed between them [21]. It can also be measured by using a monochromatic light source and photoelastic modulators (PEM). A photoelastic modulator uses the photoelastic effect, that a transparent solid material can be birefringent from mechanical forces, to either modulate the polarization of light going through it or be used as an analyzer to detect the polarization of light [22][23]. The advantage with using a PEM is that since it modulates the polarization of light, information can be obtained for all directions.

3
Methods

In this chapter, the preparation of the used suspensions and the experimental setup is described, followed by the performed data analysis.

3.1 Sample preparation

1 wt% caroboxymethylated cellulose nanofibril suspension was provided by RISE, Sweden. Three concentrations of CNF suspensions were studied in this project 0.1 wt%, 0.25 wt% and 0.5 wt%. The desired concentrations were made from the 1 wt% suspension of CNF by dilution. The required amount of CNF suspension and Milli-Q water was measured to a beaker by weight. Then the mixture was put on a magnetic stirrer for at least 3 and 6 hours until they were well homogenized for the lower (0.1 and 0.25 wt%) and higher concentrations (0.5 wt%), respectively. While a suspension was stirred the beaker was covered by parafilm to prevent evaporation. After the necessary time of mixing, the suspension was transferred from the beaker to closed containers. The vials were kept in a fridge until the measurement.

An image with three vials of a 0.25 wt% suspension from the same batch, is shown in Figure 3.1

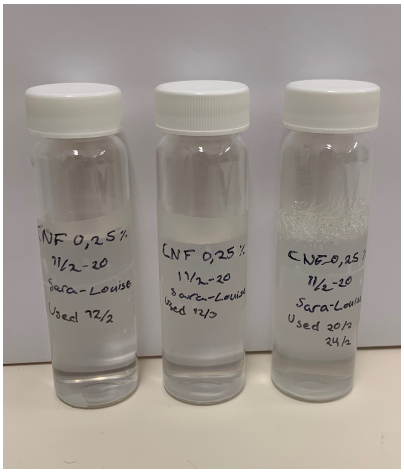

Figure 3.1: Three vials containing 0.25 wt% CNF suspension from a batch that was made 2020-02-11.

3.2 Setup and measurements

The FFoRM device consists of a metal plate and two PMMA cover layers, which are held together with 3M Adhesive Transfer Tape 468MPF. The center of the device, where the measurements are performed is cut to avoid the signal of the plastic in the measurement. The holes are covered with mica layers to seal the device. The setup used to measure the birefringence of the CNF suspensions is shown in Figure 3.2. It consists of the Exicor Birefringence MicroImager on the left in the image with the FFoRM device where the sample is placed in the microscope and then the tubes connecting between the FFoRM device, the pumps and the suspension. Both the inlet and outlet tubes are placed in the vial with the sample allowing continuous measurements. For all measurements the same length and type of tubes were used. Four milliGAT pumps were used, one for each inlet in the FFoRM device. The pumps were connected to the FFoRM device in pairs so that the opposing channels were controlled to have the same flow rate. The pumps were controlled by a computer on the side with a LabVIEW control software where the desired flow rates for each of the pumps and therefore in the inlets could be typed in (in units of µL/s).

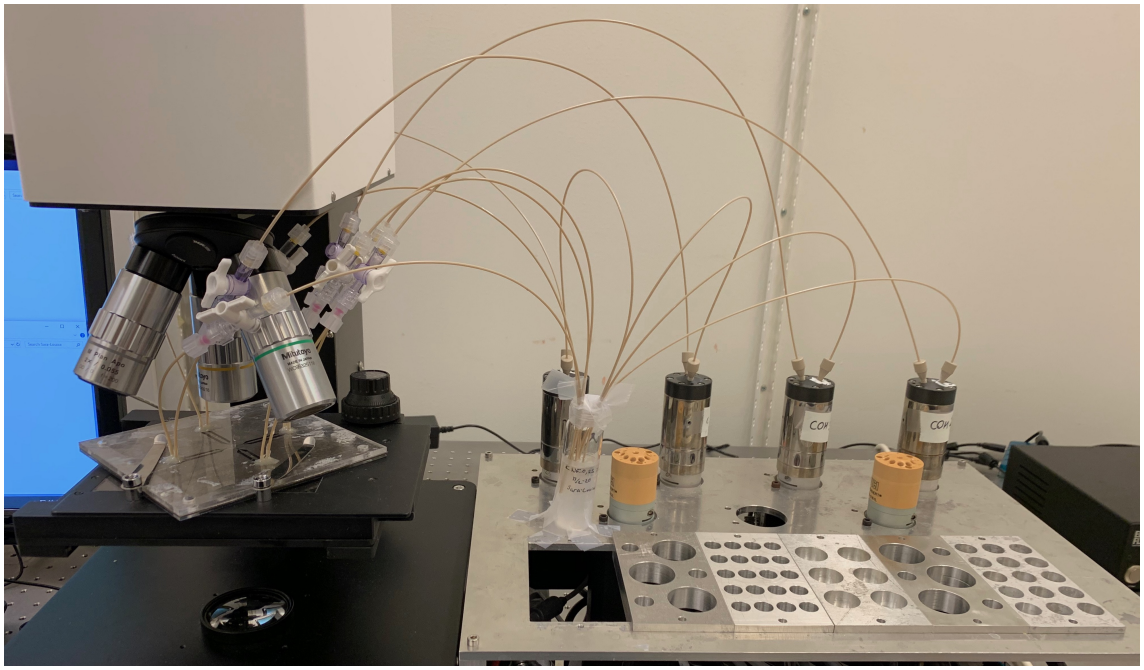

Figure 3.2: The setup used for the experiments with the Exicor Birefringence MicroImager, the FFoRM, the vial with CNF suspension, the pumps and the tubes connecting everything.

After the filling of the device, a flow type and flow rate was set. Ten datasets were recorded with the chosen set of parameters by four LEDs (red: 655 nm, orange: 615 nm, green: 535 nm, blue: 475 nm). The flow types studied were extensional flow ($Q_2 = -Q_1$), shear flow ($Q_2 = 0.8 \cdot Q_1$), a mixed flow type with $Q_2 = 0$ and another mixed flow type with $Q_2 = 0.55 \cdot Q_1$, where Q_1 and Q_2 are the flow rates in the channels of the FFoRM. Five (Q_1) flow rates were measured for each concentration and flow type: 1 µL/s, 5 µL/s, 10 µL/s, 20 µL/s and 50 µL/s. When

all the flow rates for one flow type was measured the flow type was changed and the same measurements were made.
After each day of measurement or when a different concentration of suspension was to be used the system was cleaned by Milli-Q water and air.

3.3 Data analysis

From the measurements, data was obtained in the form of images and raw binary files with information about the intensity, angle of the fast axis and retardance. The data analysis was then done with Python scripts, in three steps. The first step was to rearrange the data into three matrices of size 2048×2048 pixels with values of the intensity, angle of the fast axis and retardance in each pixel. It was followed, in the second step, by determining the position of the stagnation point by finding the symmetry center of the field of view. This pixel was then used as the center for an area (10×10 pixels) in which the averages and standard deviations of the values of the intensity, angle and retardance were calculated. These values were then plotted against the number of dataset. This way the presence of any dirt or a bubble that had appeared and disturbed the measurement could be found and removed from further calculations. The values corresponding to the measured parameters were taken as the average of all the disturbance-free datasets.
In case of the angle, the averages and standard deviations were calculated as a circular average and circular standard deviation between $-\pi/2$ and $\pi/2$. The error, E_{final}, for the final averages, μ_{final}, was calculated as

$$E_{\text{final}} = \sqrt{\sum_{i=1}^{n} \left(\frac{E_i}{\mu_i}\right)^2} \cdot |\mu_{\text{final}}| \quad \text{with} \quad E_i = \frac{\sigma_i}{\sqrt{m}}, \tag{3.1}$$

where n is the number of datasets used for the average, μ_i is the average for dataset i, σ_i is the standard deviation for dataset i and m is the number of pixels in the square that was used for the averages of each dataset [24].

3.4 Rheology

Dynamic frequency and strain sweep characterizations were performed on the TA Instruments ARES G2, New Castle, DE, USA, Anton Paar MCR702 TwinDrive, Graz, Austria. Plate-plate 25 mm and 50 mm geometries were used for the higher ($\geq$ 0.5 wt%) and lower ($<$ 0.5 wt%) concentration suspensions, respectively, with gap setting of 1 mm. All rheological tests were conducted at room temperature. The samples, without any preshearing, were loaded into the device and allowed to equilibrate for five minutes before the measurements began. Strain sweep measurements of the storage (G') and loss moduli (G'') were conducted at $\omega = 10$ rad/s 0.05–200 % range. A strain amplitude of 1%, within the linear viscoelastic regime, was chosen for frequency sweep measurement in the range of 0.08–600 rad/s.

4

Results and discussion

This chapter presents and discusses the results that were obtained from the performed measurements as described in Chapter 3. First the rheology results are presented and then follow the results from the measurements with the birefringence imager comparing the different concentrations of suspensions, flow rates and flow types.

4.1 Rheology

The rheological properties of the studied suspensions were characterized by frequency sweep and strain sweep measurements. In Figure 4.1 the resulted viscosity and dynamic moduli are shown.

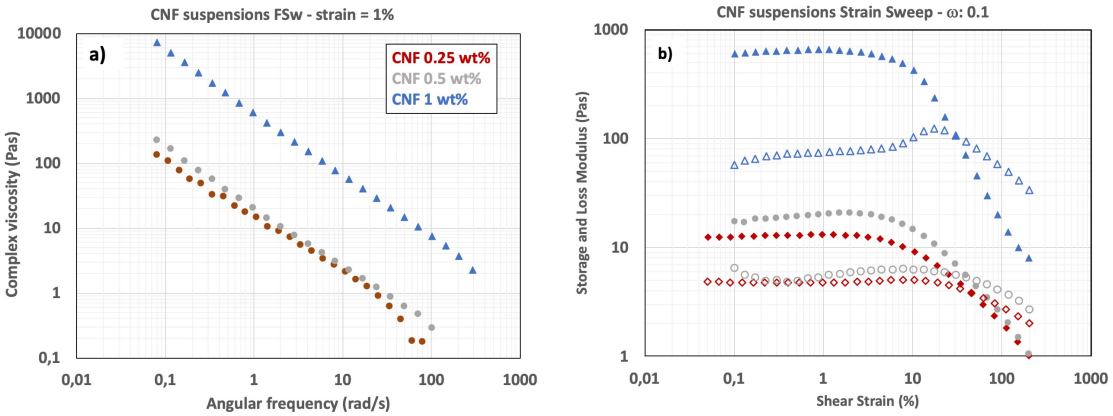

Figure 4.1: Rheological measurements of CNF suspensions. a) concentration dependence of complex viscosity determined by frequency sweep measurement and b) strain sweep measurements with solid and hollow symbols belonging to the storage and loss modulus values, respectively.

Figure 4.1 a) shows that the viscosity of the CNF suspensions depend strongly on the concentration. The viscosity is lowest for the 0.25 wt% suspension, slightly higher for the 0.5 wt% suspension and significantly higher for the 1 wt% suspension. The results from the strain sweep measurements, in Figure 4.1 b) show that the suspensions behave like a physical gel, but it is also seen that the loss modulus has a small increase, the so called weak strain overshoot, in the 0.5 and 1 wt% suspensions. Following the linear viscoelastic regime, the storage modulus decreases continuously, while the decrease in the loss modulus occurs only after a small increase. This can

be explained by structure that is built up breaking down here [25]. This bump was not visible in the lower concentration (0.25 wt%), while concentration increase, e.g. more interactions in the suspensions make it more visible. Therefore, it can be assumed that the 0.5 as well as the 1 wt% suspension are already dominated by interactions and thus in the concentrated regime, while the 0.25 wt% suspension is semi-dilute where interactions are important but not dominating the behaviour of the system. The lowest chosen concentration (0.1 wt%) for this study was not measured with the same rheological setup, because its viscosity is too low. However, it can be assumed that it is in the dilute regime.

4.2 Flow fields in the FFoRM

Figure 4.2 shows typical images of what the different flow types looked like in the FFoRM device with the birefringence imager. a), b) and c) show the intensity, angle of the fast axis and retardance, respectively, for the extensional flow type ($Q_2 = -Q_1$). d), e) and f) show the same information for the extensionally dominated mixed flow ($Q_2 = 0$), g), h) and i) for the shear dominated mixed flow ($Q_2 = 0.55 \cdot Q_1$) and j), k) and l) for the pure shear flow ($Q_2 = 0.8 \cdot Q_1$) [8]. The data for these images were recorded with the microscope, plotted with a Python script and used for the data analysis. All of these images are taken from measurements with a 0.25 wt% suspension, with flow rate $Q_1 = 20\,\mu L/s$ and red LED.

4.3 Colour of LED

Figure 4.3 shows the retardance values extracted from a) extensional flow and b) shear flow using 0.25 wt% suspension and all four colours of LEDs in the birefringence imager.
Based on the examples shown in Figure 4.3 the retardance values measured with the different colours or wavelengths of the LEDs, are very similar. There is only a small difference (maximum 10 nm), which could be caused by choosing manually the center point or small differences in the focal point of the microscope. This result shows that performing measurements with different wavelengths of the LEDs, give similar enough results so that it is enough to only use one LED for measurements. In the rest of the results, results obtained with only the red LED are shown.

4.4 Time effect

Measuring all the different experimental parameters took between one and four hours. In order to make sure that the continuous flow doesn't affect the measured values the effect of time on the retardance was checked. The two extremes, pure extensional and pure shear flow was studied for two hours. The flow rate was chosen to be $Q_1 = 20\,\mu L/s$, because based on Figure 4.3 it is already enough to have a significant effect on the alignment. These measurements were performed on the 0.25 wt% suspension.

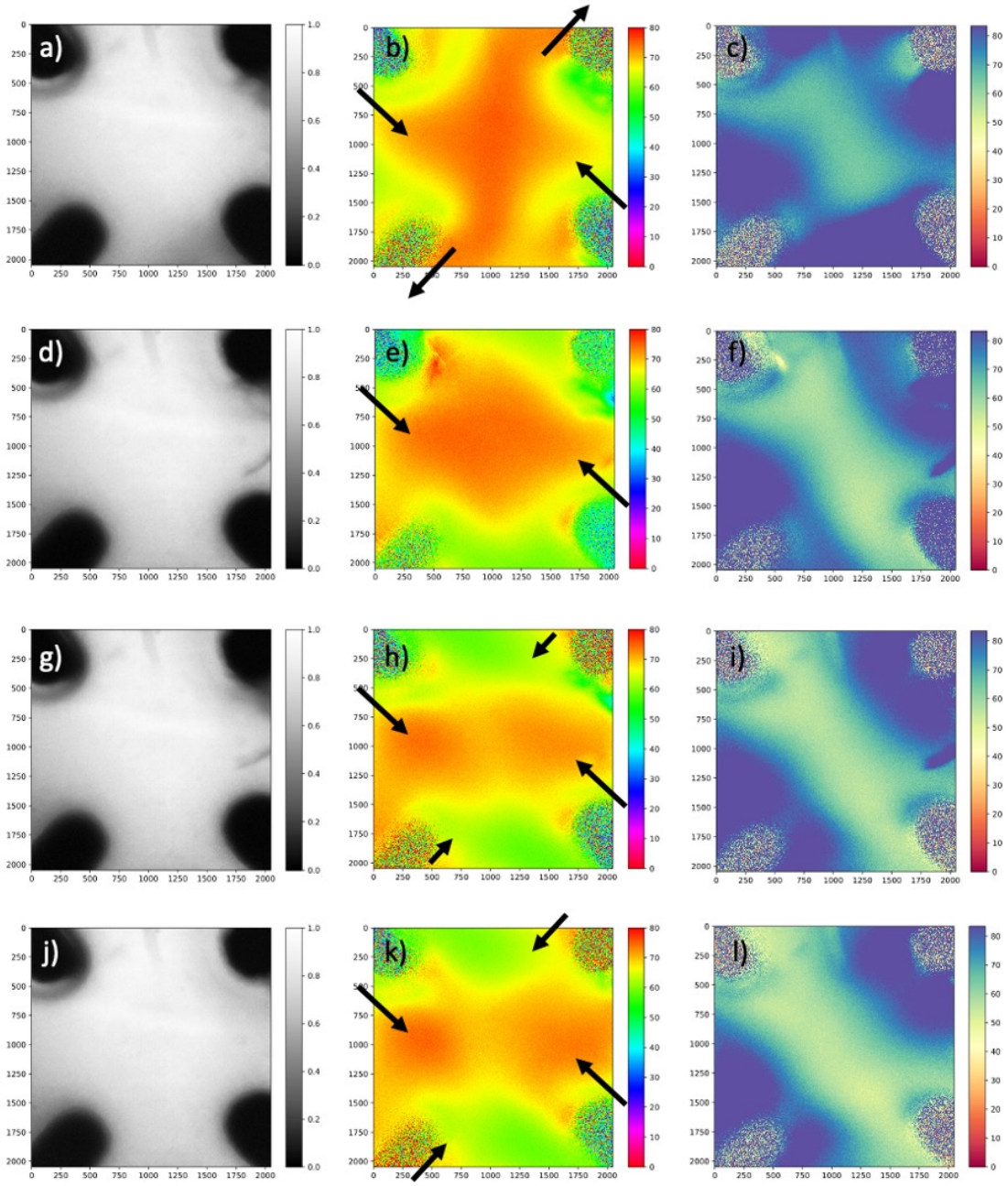

Figure 4.2: Examples of the different flow types in the FFoRM, measured with the birefringence imager. The first column (with a), d), g) and j)), shows the intensity, the second column (b), e), h) and k)) the angle of the fast axis and the third column (c), f), i) and l)) the retardance. Different rows show the different flow types, a), b) and c) extensional flow, d), e) and f) extensionally dominated, g), h) and i) shear dominated and j), k) and l) pure shear flow. The arrows in the angle images indicate the direction of flow and their length the relative flow rates, for the different flow types.

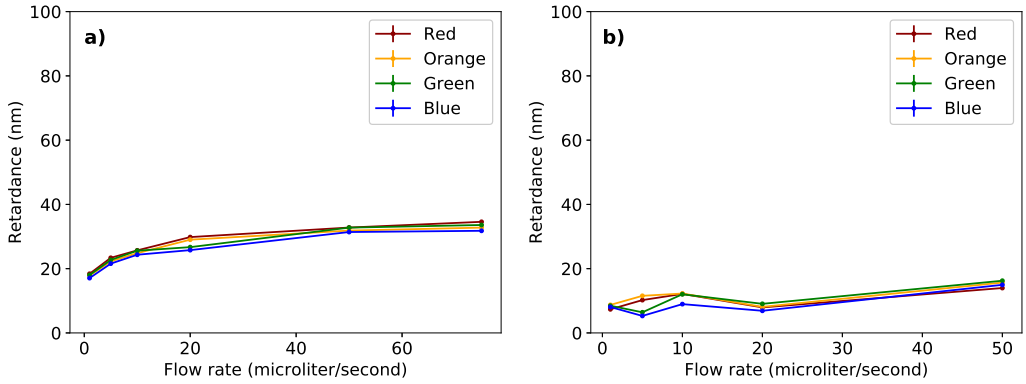

Figure 4.3: Example of measurements done with a) extensional flow and b) shear flow, with the retardance values plotted against the flow rate, measured with all four colours of LEDs available in the birefringence microscope, as indicated in the legends.

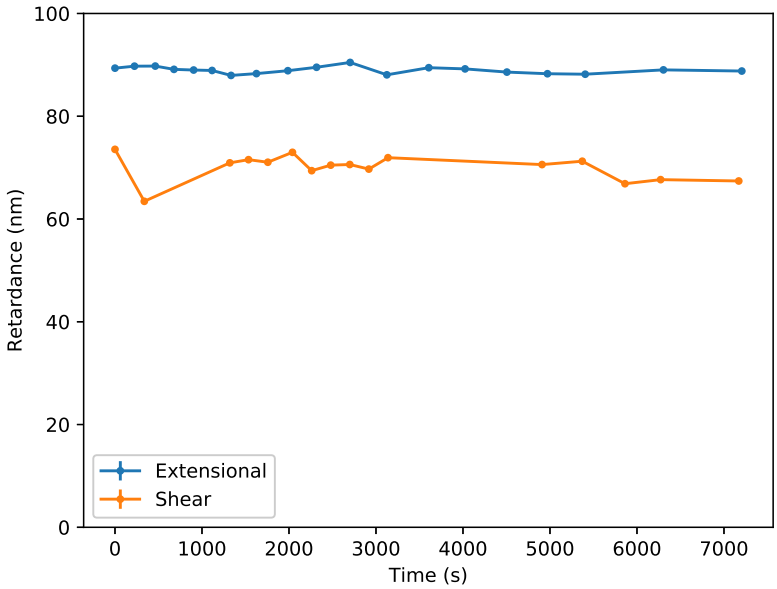

Figure 4.4: Retardance values plotted against the time of the measurement, for extensional and shear flow with $Q_1 = 20\,\mu L/s$ and a 0.25 wt% suspension.

In Figure 4.4, the retardance seemed to be relatively constant with time, for both flow types, especially for the extensional flow. The larger variations in the shear flow is probably caused by bubbles, which was more of a problem in the measurement with this flow. This result show that continuous measurements can be performed, and that the retardance values will not change significantly during the measurements.

4.5 Concentration

The concentration dependence is illustrated in Figure 4.5. Figure 4.5 shows the retardance values plotted against the concentration of the CNF suspensions, for a) extensional flow, b) extensionally dominated flow, c) shear dominated flow, and d) pure shear flow, all measured at flow rate $Q_1 = 20\,\mu L/s$.

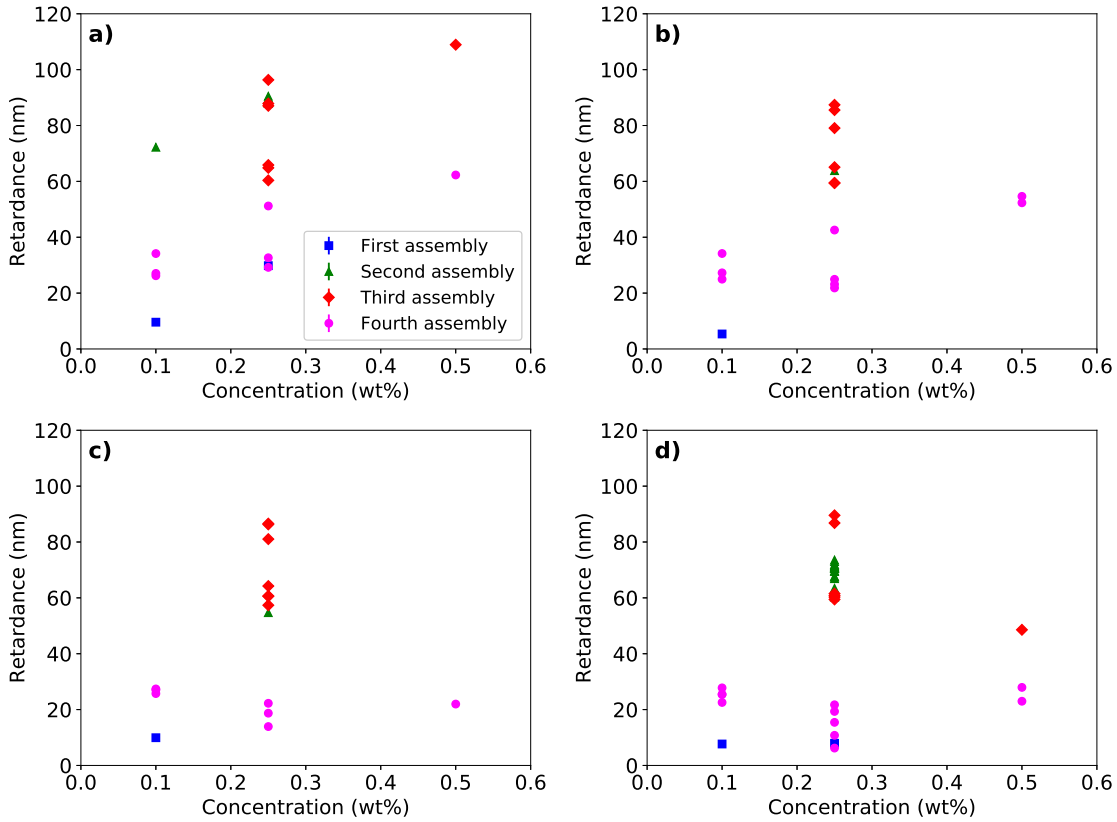

Figure 4.5: The concentration dependence of the CNF suspensions with retardance values plotted against the concentration of the suspensions, for a) extensional flow, b) extensionally dominated flow, c) shear dominated flow, and d) pure shear flow. Different assemblies of the FFoRM device are marked with different colours and markers.

Different assemblies of the FFoRM give quite different retardance values, so they should be considered separately. Looking at each assembly, for example the fourth assembly with pink circles, one can observe that the concentration dependence is different for the different flow types. For extensional flow in a), the retardance seems

to be increasing, it is at least clear that the 0.5 wt% suspension shows higher retardance values than the 0.1 wt% and 0.25 wt% suspensions. Similarly the retardance seems to be increasing with higher concentration for the extensionally dominated flow in b), though a little bit smaller increase than with pure extensional flow. For shear dominated flow, c), and pure shear flow, d), the retardance looks relatively constant and does not increase with increasing concentration.
Increased retardance was expected for higher concentrations regardless of the used flow type, due to the increased amount of fibers in the field of view. This would suggest a linear trend for the concentration dependence because the retardance for more particles sum up. However, differences were seen for the studied flow types, which means that the change in the retardance is affected more by the alignment differences and less by the concentration increase.
In the higher concentrations of the suspensions the interactions between the fibrils are more important. These results would therefore suggest that more interactions help to increase the alignment in the material in extensionally dominated flow types, but does not increase the alignment in flow types that are dominated by shear flow. Edwards et al. showed that, comparing an unentangled and entangled gel in extension, the entangled gel showed more birefringence than the unentangled gel [26]. This could be explaining the concentration dependence that is seen in the extensional flow types here, that entanglement promotes alignment in extension.
What causes the difference in the values between different assemblies of the FFoRM is not fully understood yet. The FFoRM was cleaned and assembled in the same way and with the same materials every time it was disassembled. One way to avoid this problem would of course be to do all the measurements in the same assembly of the device. Otherwise one could do background or reference measurements, for example with the empty device or filled with water or the suspension but not in flow, to see how the values might change.

4.6 Flow rate and flow type

Extensional flow was thought to be the most straight forward way to see the flow rate dependency, because based on the literature, this flow type was expected to show the largest differences in the alignment of the systems [16]. The resulted retardance, intensity and angle values are shown in Figure 4.6, which shows extensional flow measured in the fourth assembly of the FFoRM. The intensity is directly controlled during the measurements by the LED intensity. The fact that the experiments did not show significant changes proves that no bubbles or aggregates were present in the stagnation point, where the analysis was performed. The measured angle values depend on the chosen region of interest in the microscope and the specific orientation of the device, which was always set up manually. This means, that the values cannot be compared quantitatively without comparing the precise position of the channel in different images, however, the constancy of the values show the stability of the flow field independently of the applied flow rates. As opposed to the intensity and the angle values, the retardance depends on the applied flow rates.
In Figure 4.6 the flow rate dependence of the retardance looks to be different for the different concentrations. For the higher concentration, 0.5 wt%, the retardance,

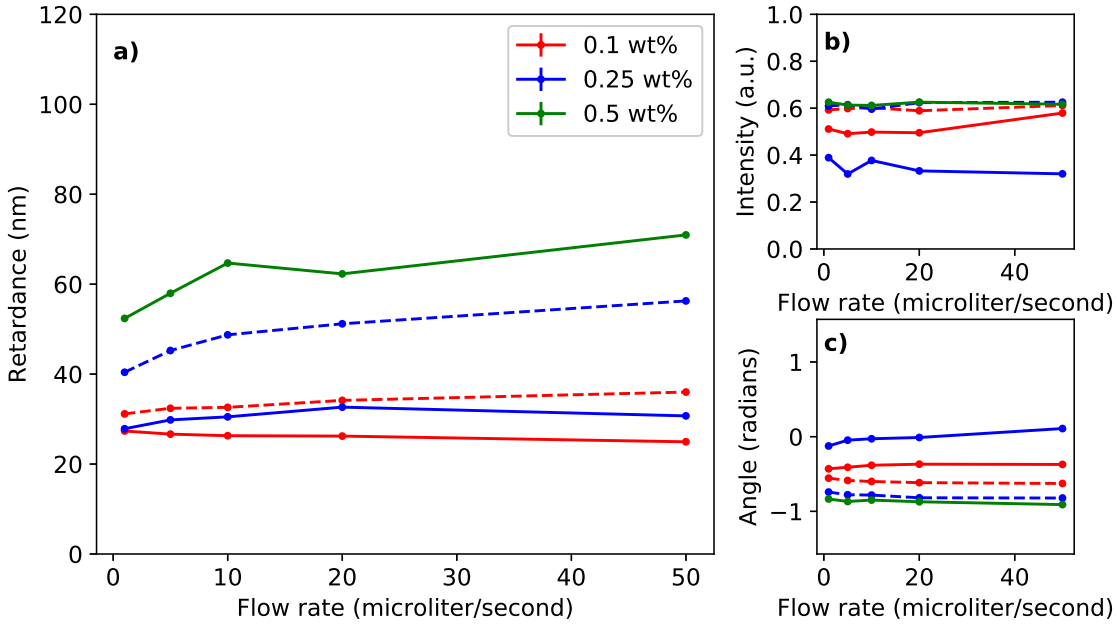

Figure 4.6: The flow rate dependence for CNF suspensions in extensional flow, plotted for the fourth assembly of the FFoRM device. The retardance is plotted against the flow rate in a), the intensity in b) and the angle of the fast axis in c). The solid lines show the first measurements on a new vial, the dashed lines are second measurements of the same vial, measured on the same day as the 0.5 wt% suspension was measured.

and alignment, looks overall increasing with higher flow rates. However for the 0.25 wt% concentration it seems a bit more unclear. The solid blue line, for the first measurement of a vial with 0.25 wt% suspension, does not show much dependence on the flow rate, but the dashed line for the second measurement of the same vial shows a clear increase. This could maybe be caused by an aging effect in the suspension, which could mean that aging also affects the flow rate dependence of suspensions with this concentration. For the lowest concentration, 0.1 wt%, there is no clear dependence of the retardance values in either the solid red line or the dashed red line. There might be a small increase in the dashed line with increasing flow rate, but it is still significantly smaller than the increase shown for the higher concentration. This apparent difference in the flow rate dependence of the different concentrations can be attributed to the different concentration regimes, e.g. diluted, semi-dilute and concentrated. This would suggest that the flow rate dependency is influenced by the amount of interactions in the suspension.

A possible explanation for this increase in retardance with increasing flow rate for the 0.25 wt% concentration and not for the 0.1 wt% concentration could be attributed to the entangled networks being more stretched in higher flow rates of extension, inducing more alignment. In the dilute regime the lack of entanglement doesn't increase the alignment significantly.

To investigate the combined effect of the flow type and the flow rate on the semi-dilute, 0.25 wt%, and the dilute, 0.1 wt%, suspensions were used. Figure 4.7 shows the flow rate dependency with extensionally dominated mixed flow, shear dominated mixed flow and pure shear flow. These were not all measured in the same assembly of the FFoRM device, so the values are not directly comparable, but the trends can be determined. The two mixed flow types were measured in the first assembly and the pure shear flow type in the second assembly.

The intensity values are relatively stable, as it was seen for the extensional flow as well. The angle values seem to be constant for the mixed flow types, but it was less stable for the shear flow. Here the flow rate dependency seems to suggest that the retardance, and thus the alignment, is relatively constant in the extensionally dominated mixed flow, slightly decreasing in the shear dominated mixed flow, and possibly increasing for the pure shear flow. In case of the shear flow, the results are inconclusive due to the instability of the flow. These experiments need to be repeated for a clear conclusion. It was also expected that the pure shear flow and the shear dominated flow type would behave more similarly.

In Figure 4.8 the retardance, intensity and angle are plotted against the flow rate for all of the studied flow types measured with a 0.1 wt% suspension. These were all measured in the same assembly of the FFoRM. This result shows very little change of the retardance with increasing flow rate for all the flow types. The alignment in 0.1 wt% CNF suspension therefore does not seem to be significantly influenced by the flow rate, nor the flow type. This can be attributed to the lack of interactions between the nanofibers.

As it was shown before, the measured values depend strongly on the assembly it was measured in. In order to clarify the flow type effect, in Figure 4.9, normalized retardance values are plotted against the day of measurement for all the studied flow types: extensional flow, extensionally dominated mixed flow, shear dominated

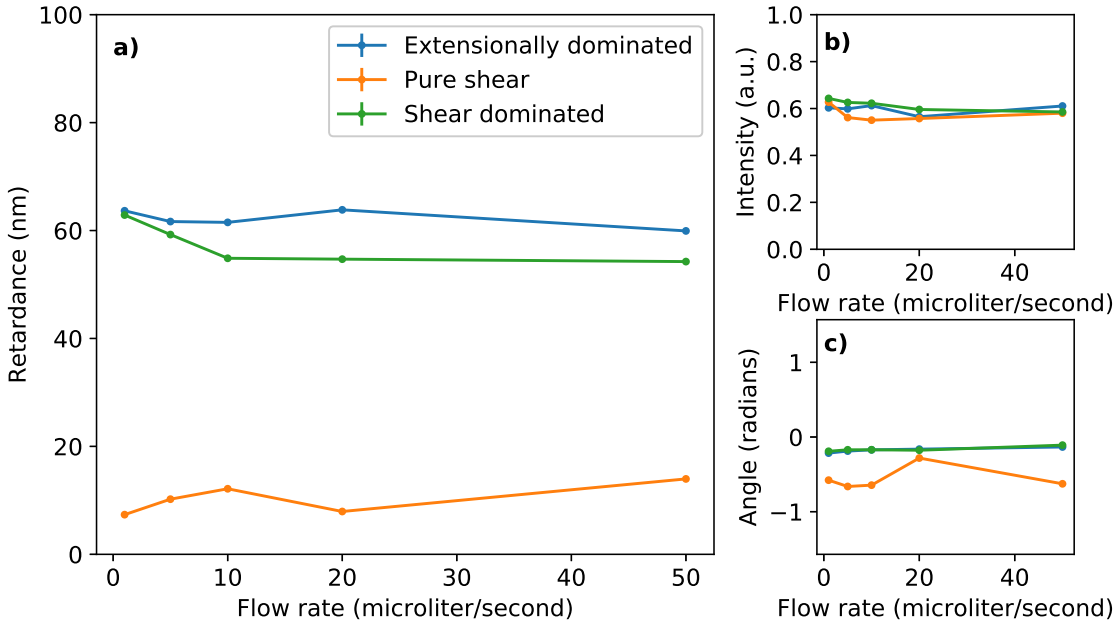

Figure 4.7: The flow rate dependency for a 0.25 wt% suspension in extensionally dominated flow, shear dominated flow and pure shear flow. Retardance is plotted in a),intensity in b), and angle of the fast axis in c).

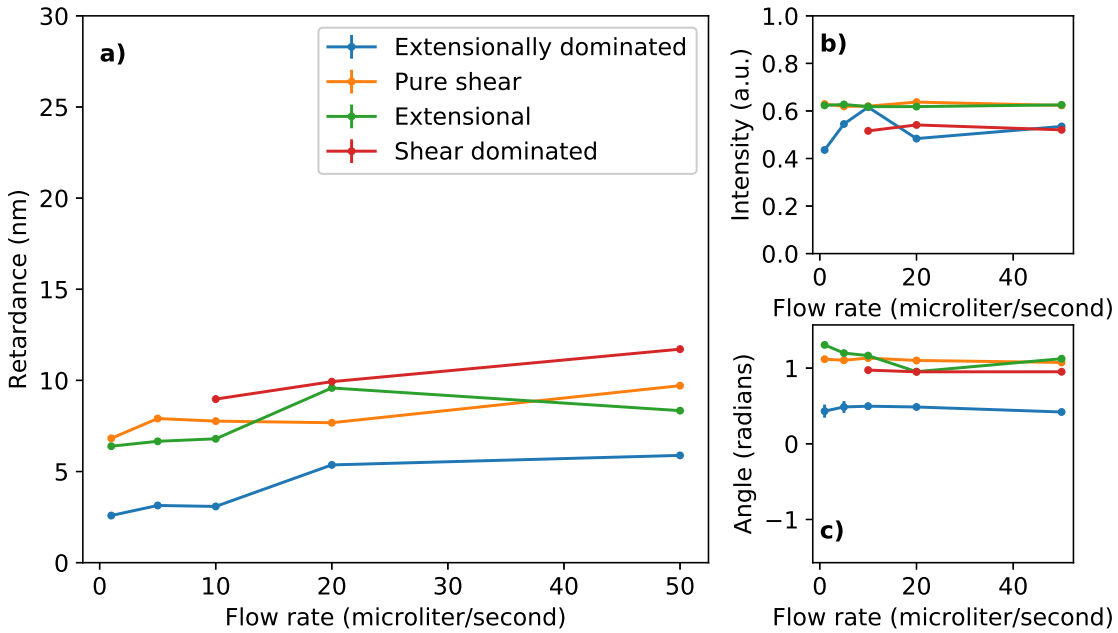

Figure 4.8: The flow rate dependency for a 0.1 wt% suspension in extensional flow, extensionally dominated mixed flow, ratio shear dominated mixed flow and pure shear flow. Retardance is plotted in a), intensity in b), and angle of the fast axis in c).

mixed flow and pure shear flow. The retardance values were normalized by their respective values of the extensional flow for each day. The compared measurements were done with flow rate $Q_1 = 20\,\mu L/s$ and concentrations 0.25 wt% in a), 0.1 wt% in b) and 0.5 wt% in c).

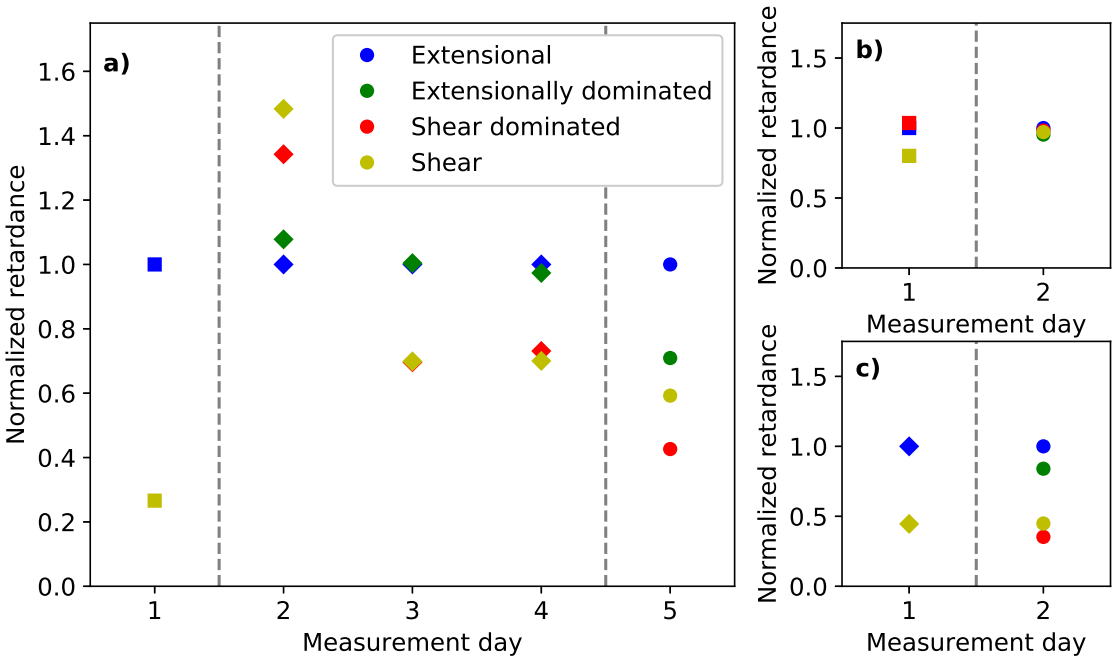

Figure 4.9: Normalized retardance values plotted for different measurement days, only for measurements that are the first measurements with a vial, for all the studied flow types, extensional flow, extensionally dominated mixed flow, shear dominated mixed flow and pure shear flow. In a) with 0.25 wt%, b) 0.1 wt% and c) 0.5 wt%. Measurements in different assemblies of the FFoRM have different markers and are separated by the vertical lines.

In Figure 4.9 a) one can see that, except for the second day, the extensional flow (blue) is always higher than the shear flow (yellow). This implies that extensional flow is better at aligning the nanofibrils than shear flow in the 0.25 wt% suspensions. In Figure 4.9 b) for the 0.1 wt% concentration, the points are closer together, indicating that the flow type does not influence the alignment significantly in this concentration. Though in the first day plotted the yellow point, pure shear, is a bit lower than the other ones. For the highest concentration, 0.5 wt%, in Figure 4.9 c), the extensional flow show higher values than the pure shear flow for both days, again implying that extensional flow is more effective for aligning the fibers than shear flow. The reason for this difference between extensional and shear flow can be that the fibrils are stretched out in extensional flow, but in shear flow there is also some rotation that can cause the fibrils to flip and maybe curl up [27].
It is harder to say in what order the two mixed flow types are. The difference between the flow types also varies quite a lot between different days, this difference might be caused by the measurements being done in different assemblies of the FFoRM, as separated with the vertical lines and markers in Figure 4.9.

The slight difference in these plots between the concentrations, also hints at a possible dependence on concentration or interactions between the fibers. The flow type might have more importance on the alignment in the higher concentrations, but not in the lowest measured concentration.
In, for example, the fourth day plotted in Figure 4.9 a), the order of the flow types is in decreasing order, extensional flow, extensionally dominated flow, shear dominated flow and pure shear flow. This was the expected order of the flow types, since previous studies show that extensional flow is very effective for alignment [16]. It is hard do determine based on this data, since for example in the second day plotted in Figure 4.9 the flow types show the opposite order. It is clearer in higher concentrations (0.25 and 0.5 wt%) that the flow type influences the alignment, but the flow types have no significant effect in lower concentrations like 0.1 wt%.

4.7 Age of suspension, measurement effect and sample batch

As the project advanced, it seemed that the assembly is not the only parameter that one needs to take into account. Using the same suspension under the same conditions, even in the same assembly, different values were measured on different days. To identify the cause of these changes, a new set of experiments were performed using different vials of the same batch (e.g. a dilution produced together, then divided into several sample holders), and measuring the retardance on the exact same vial. Figure 4.10 shows plots of the retardance values against the age of the samples, with different batches and vials of 0.25 wt% suspension. Extensional flow in a), extensionally dominated mixed flow in b), shear dominated mixed flow in c) and pure shear flow in d), all measured with flow rate $Q_1 = 20\,\mu L/s$. Different colours correspond to different batches and different shades to distinct vials from that batch. The connected points show repeated measurement on the same vial.
Regarding the age of the samples, it seems that the retardance, or alignment in case of the extensional flow type is first increasing and reaching a peak within the first five days. This is then followed by either a constant high retardance value or a small decrease. More points of "older" samples are needed to clarify the tendency. The dark green circle is an outlier, e.g. the measured retardance doesn't show age dependency. It can be attributed to the fact that the two points were measured in different assemblies. Upon repeated measurement in the first five days, the retardance increases, while for older samples it decreases. In case of the two mixed flows, the observed trends are similar, but the slope of the lines are different, so there is a difference in the effect of measurement or aging of the samples depending on the flow type. Another observation that can be made, when comparing the light blue and light green lines, is the effect of the distinct batches. Quantitatively the values are not exactly the same, but they are very similar for all of the flow types. Even if one would measure the same sample, there would be numerical differences between the resulted values, most probably due to polydispersity of the samples and the (yet) uncontrolled parameters. Based on this, the difference between batches has a smaller effect on the measured values than other parameters, therefore, results and

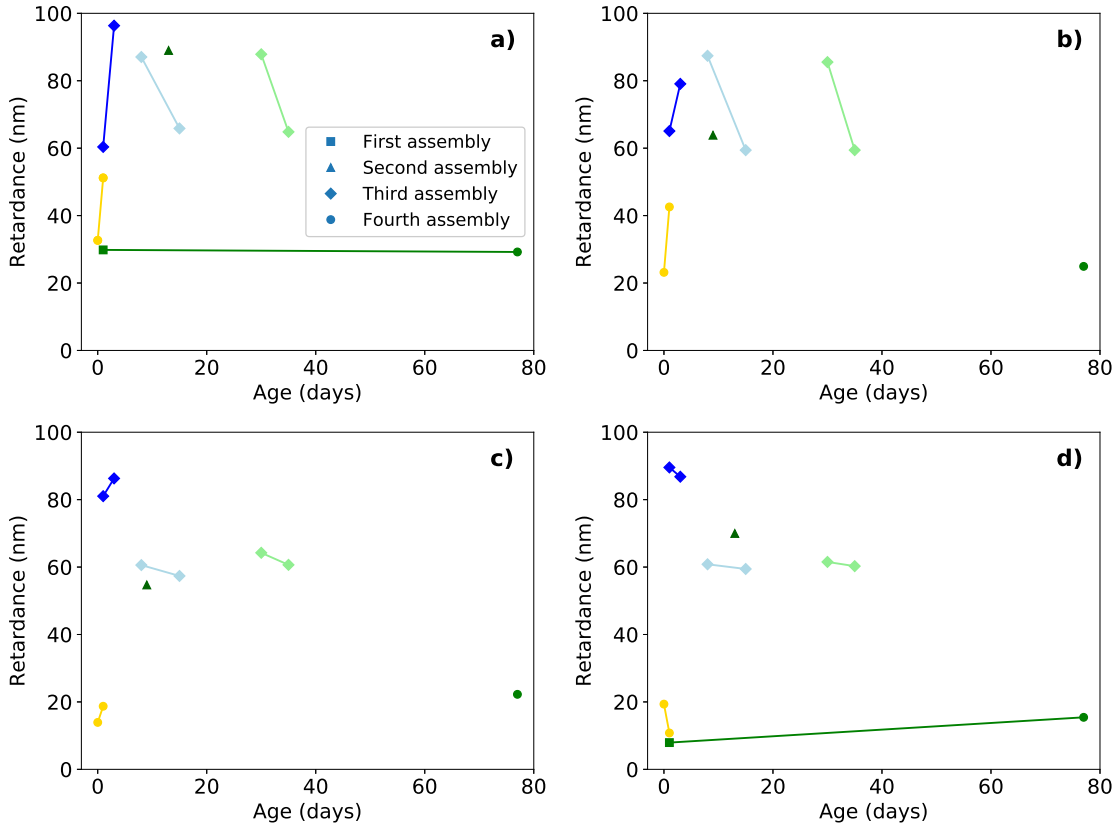

Figure 4.10: Aging data of 0.25 wt% CNF suspensions, showing the retardance values plotted against the age of the suspensions, in days. Different colours correspond to different batches, and different shades to different vials. a) is extensional flow, b) extensionally dominated mixed flow, c) shear dominated mixed flow and d) pure shear flow. Points that was measured in different assemblies of the FFoRM have different markers.

trends observed for different batches can be confidently compared.
In case of the shear flow, any repetition done resulted in a lower retardance value than the one measured before. It could mean either that the differences measured in shear flow are so small, that we cannot deem them significant, or this flow type is the least sensitive to the flow-history of the studied material. More measurements are needed to determine which explanation is right.
The complex behaviour of the observed alignment in the suspensions could be attributed to networks forming and breaking apart in the material. First, directly after preparation of the sample, there is probably no network and the material is broken up due to the mixing the suspension faced during the dilution. Then as time passes from the preparation a network starts forming, and from this data, it seems that after maybe 5-7 days the material is the most entangled it can be, the system reaches some sort of equilibrium. This system is probably in a dynamic equilibrium, therefore numerical differences can be observed during measurements on a later day. As mentioned above, further experiments are needed to gain information on the "older" samples. During a flow experiment, the sample faces quite a bit of shear or extension, which is very likely to influence the equilibrium structure, by breaking it up. This effect is less impactful than the dilution was, since the retardance values do not decrease back to the starting values. The structural changes can be either fracture of fibers or rearrangement of the built up network. This can be determined by measuring the same vials again after 5-7 days of waiting time in the same assembly. If the system is able to get back to the same equilibrium as before, high retardance values can be measured again, if not, the flow experiments potentially can cause irreversible structural changes too.

5

Conclusion and outlook

5.1 Summary and conclusions

The purpose of this thesis was to study the effect of complex flow fields on cellulose nanofibril suspensions with birefringence imaging. Three different concentrations of the suspensions, one in the dilute, one in the semi-dilute and one in the concentrated regime, were studied, in four different flow types and five different flow rates. The fluidic four-roll mill was used to create the different flow fields, and the alignment was then determined by measuring the retardance in a birefringence imager.

In this project it was found that the used method and setup, with the FFoRM device and a birefringence imager, can be used for measuring the retardance or alignment in CNF suspensions, with some limitations. Tests were done to see that any colour of LED can be used in the birefringence microscope and one can do continuous measurements without the retardance values changing significantly. The alignment in the material was found to depend on the concentration, flow rate, flow type and possibly also the age of the suspensions. From the results these main conclusions can be drawn:

- It seemed that the alignment of the fibers increased with higher concentration, e.g., more interactions between the fibers, in the extensional and extensionally dominated flow types. However, in the pure shear and shear dominated flow types, increased concentration did not affect the alignment.
- There was also differences between the dilute, semi-dilute and concentrated concentration regimes in the flow rate dependency. In case of the extensional flow, the alignment increased with increasing flow rate in the highest concentration, but the flow rate did not seem to increase the alignment in the lowest concentration. With the 0.25 wt% concentration the flow rate dependence of the alignment is either increasing or constant, seemingly depending on the age of the sample. The flow rate dependence of the alignment in the other flow types with this concentration is unclear, more measurements are needed. With the lowest concentration (0.1 wt%) neither the flow types or the flow rates seem to have effect on the alignment.
- It seems that the alignment is higher with extensional flow than with shear flow, with the two higher concentrations.
- The results also showed a possible aging effect that could be attributed to networks forming and breaking in the suspension.

These results therefore suggest that a higher concentration suspension should be used that is in the concentrated regime, with extensional flow and at a high flow

rate in order to achieve the highest alignment.
The found results agree with literature in showing that entangled systems like the higher concentration suspensions seem to show more alignment in extension than unentangled systems [26]. They also agree with literature in showing that extensional flow is more effective in increasing alignment in these suspensions than shear flow [16], but also seem to show a possible aging dependence. It was expected maybe to also see increased alignment in all flow types in higher flow rates [6], however here those results are a bit more unclear and would need to be repeated.

5.2 Outlook and problems

For future experiments it could be interesting to combine this method, using the FFoRM and birefringence imager, with other measurement methods such as scattering methods for structural properties and rheo-optical setups for example. Particle tracking measurements using glass beads (PIV or PTV), could also be done to confirm the flow properties, the glass beads would probably influence the interactions in the suspensions. To widen the flow rate range different pumps could be used, to also be able to measure higher concentrations of the suspensions. Different samples could also be used for new measurements, for example suspensions with controlled aspect ratio or from different starting sources.
The main problems that occurred during the measurements were the difference in retardance values seemingly between different days, and the problem with bubbles and dirt in the samples that disturbed the flow. Bubbles and dirt in the sample suspension or the FFoRM could make the flow unstable in the measurements. The bubbles were also more of a problem in the higher concentration of suspension that was used since they were more viscous than the lower concentrations. Bubbles that appeared in the system during these measurements were more likely to stay in the suspension in case of higher viscosity. Eventually there were too many bubbles in the suspension that made it difficult to get stable measurements. This problem could be fixed maybe with a bubble trap of some kind that would get rid of bubbles before the sample goes into the FFoRM. To get rid of any dirt that could disturb the flow the optimal solution would be to prepare and maybe even assemble the FFoRM and also perform the experiments in a cleanroom.
It was found that the retardance values seemed to change whenever the FFoRM device was disassembled and assembled again, so something must be changing or affecting the flow in some way. One way to get rid of the problem with different retardance values in different assemblies of the FFoRM would be to try to perform all the measurements in the exact same assembly, if possible, to completely get rid of different assemblies as a factor for the different values. Doing reference or background measurements on every measurement day could make it possible to compare measurements in different assemblies. These background measurements could be with the empty FFoRM device, of milli-Q water in the device or with the suspension in the device but not in flow. In the analysis these measurements could be used to clarify the effect of the sample in the different flow fields.

Bibliography

[1] Sveaskog. *What is Swedish forestry?* https://www.sveaskog.se/en/forestry-the-swedish-way/short-facts/brief-facts-1/. Accessed: 2020-04-23.

[2] Knut and Alice Wallenberg Foundation. *Swedish forest can be converted into new environmentally friendly super material.* https://kaw.wallenberg.org/en/research/swedish-forest-can-be-converted-new-environmentally-friendly-super-material. Accessed: 2020-04-23.

[3] Hernán Charreau, Ema Cavallo, and María Laura Foresti. "Patents involving nanocellulose: Analysis of their evolution since 2010". In: *Carbohydrate Polymers* 237 (2020). ISSN: 01448617. DOI: 10.1016/j.carbpol.2020.116039.

[4] Sahar Sultan et al. *3D printing of nano-cellulosic biomaterials for medical applications.* June 2017. DOI: 10.1016/j.cobme.2017.06.002.

[5] Pezhman Mohammadi et al. "Aligning cellulose nanofibril dispersions for tougher fibers". In: *Scientific Reports* 7.1 (Dec. 2017), pp. 1–10. ISSN: 20452322. DOI: 10.1038/s41598-017-12107-x.

[6] Tomas Rosén et al. "Orientation Distributions of Cellulose Nanofibrils and Nanocrystals in Confined Flow". In: *ChemRxiv, Preprint* 2 (May 2019). DOI: 10.26434/chemrxiv.8150717.v1.

[7] Christophe Brouzet et al. "Characterizing the Orientational and Network Dynamics of Polydisperse Nanofibers on the Nanoscale". In: *Macromolecules* 52.6 (Mar. 2019), pp. 2286–2295. ISSN: 15205835. DOI: 10.1021/acs.macromol.8b02714.

[8] Patrick T. Corona et al. "Probing flow-induced nanostructure of complex fluids in arbitrary 2D flows using a fluidic four-roll mill (FFoRM)". In: *Scientific Reports* 8.1 (Dec. 2018). ISSN: 20452322. DOI: 10.1038/s41598-018-33514-8.

[9] Patchiya Phanthong et al. "Nanocellulose: Extraction and application". In: *Carbon Resources Conversion* (2018). ISSN: 25889133. DOI: 10.1016/j.crcon.2018.05.004.

[10] Alain Dufresne. *Nanocellulose: A new ageless bionanomaterial.* 2013. DOI: 10.1016/j.mattod.2013.06.004.

[11] Oleksandr Nechyporchuk, Mohamed Naceur Belgacem, and Frédéric Pignon. *Current Progress in Rheology of Cellulose Nanofibril Suspensions.* 2016. DOI: 10.1021/acs.biomac.6b00668.

[12] Swambabu Varanasi, Rongliang He, and Warren Batchelor. "Estimation of cellulose nanofibre aspect ratio from measurements of fibre suspension gel

point". In: *Cellulose* 20.4 (Aug. 2013), pp. 1885–1896. ISSN: 09690239. DOI: 10.1007/s10570-013-9972-9.

[13] Karl Håkansson. *Orientation of elongated particles in shear and extensional flow*. Engineering Sciences, Royal Institute of Technology (KTH), 2012. ISBN: 9789175014043.

[14] Karl M.O. Hakansson et al. "Nanofibril Alignment in Flow Focusing: Measurements and Calculations". In: *Journal of Physical Chemistry B* 120.27 (July 2016), pp. 6674–6686. ISSN: 15205207. DOI: 10.1021/acs.jpcb.6b02972.

[15] Farzan Akbaridoust, Jimmy Philip, and Ivan Marusic. "Assessment of a miniature four-roll mill and a cross-slot microchannel for high-strain-rate stagnation point flows". In: *Measurement Science and Technology* 29.4 (Mar. 2018), p. 045302. ISSN: 0957-0233. DOI: 10.1088/1361-6501/AAACF3.

[16] Tomas Rosén et al. "Dynamic characterization of cellulose nanofibrils in sheared and extended semi-dilute dispersions". In: (Jan. 2018). URL: http://arxiv.org/abs/1801.07558.

[17] Joo Sung Lee et al. "Microfluidic four-roll mill for all flow types". In: *Applied Physics Letters* (2007). ISSN: 00036951. DOI: 10.1063/1.2472528.

[18] MicroscopyU. *Principles of Birefringence*. https://www.microscopyu.com/techniques/polarized-light/principles-of-birefringence. Accessed: 2020-04-21.

[19] Hinds Instruments. *Birefringence Measurement*. https://www.hindsinstruments.com/knowledge-center/technology-primer/birefringence-primer/. Accessed: 2020-04-21.

[20] Luiza Larsen et al. "Polarized light imaging of white matter architecture". In: *Microscopy Research and Technique* 70.10 (Oct. 2007), pp. 851–863. ISSN: 1059910X. DOI: 10.1002/jemt.20488.

[21] Olympus Life Science. *Polarized Light Microscopy*. https://www.olympus-lifescience.com/en/microscope-resource/primer/virtual/polarizing/. Accessed: 2020-05-06.

[22] Hinds Instruments. *Photoelastic Modulation Principles of Operation*. https://www.hindsinstruments.com/knowledge-center/technology-primer/pem-photoelastic-modulation/principles-of-operation/. Accessed: 2020-04-21.

[23] Hinds Instruments. *Modes of Operation*. https://www.hindsinstruments.com/knowledge-center/technology-primer/pem-photoelastic-modulation/modes-of-operation/. Accessed: 2020-04-21.

[24] Chemistry LibreTexts. *Propagation of Error*. https://chem.libretexts.org/Bookshelves/Analytical_Chemistry/Supplemental_Modules_(Analytical_Chemistry)/Quantifying_Nature/Significant_Digits/Propagation_of_Error. Accessed: 2020-05-28.

[25] Fatima Fneich et al. "Structure and rheology of aqueous suspensions and hydrogels of cellulose nanofibrils: Effect of volume fraction and ionic strength". In: *Carbohydrate Polymers* 211 (May 2019), pp. 315–321. ISSN: 01448617. DOI: 10.1016/j.carbpol.2019.01.099.

[26] Chelsea E.R. Edwards et al. "Molecular anisotropy and rearrangement as mechanisms of toughness and extensibility in entangled physical gels". In:

Physical Review Materials 4.1 (Jan. 2020). ISSN: 24759953. DOI: 10.1103/PhysRevMaterials.4.015602.

[27] Tomas Rosén et al. "Flow fields control nanostructural organization in semi-flexible networks". In: *Soft Matter* (2020). ISSN: 1744-683X. DOI: 10.1039/C9SM01975H. URL: http://xlink.rsc.org/?DOI=C9SM01975H.

DEPARTMENT OF PHYSICS
CHALMERS UNIVERSITY OF TECHNOLOGY
Gothenburg, Sweden
www.chalmers.se

CHALMERS
UNIVERSITY OF TECHNOLOGY